LRP 716/01 December 2001

From current driven to neoclassically driven tearing modes

H. Reimerdes, O. Sauter, T. Goodman
& A. Pochelon

Accepted for publication in
Physical Review Letters

ISSN 0458-5895

From current driven to neoclassically driven tearing modes

H. Reimerdes,* O. Sauter, T. Goodman, and A. Pochelon

Centre de Recherches en Physique des Plasmas,

Association EURATOM - Confédération Suisse,

Ecole Polytechnique Fédérale de Lausanne, 1015 Lausanne, Switzerland

Abstract

In the TCV tokamak, the $m/n = 2/1$ island is observed in low density discharges with central electron cyclotron current drive. The evolution of its width has two distinct growth phases, one of which can be linked to a "conventional" tearing mode driven unstable by the current profile and the other to a neoclassical tearing mode driven by a perturbation of the bootstrap current. The TCV results provide the first clear observation of such a destabilization mechanism and reconcile the theory of conventional and neoclassical tearing modes, which only differ in their dominant driving term.

PACS numbers: 52.30.Cv, 52.35.Py, 52.55.Fa

*Permanent address: General Atomics, P.O. Box 85608, San Diego, California 92186-5608; Electronic address: reimerdes@fusion.gat.com

Magnetic islands arise from helical perturbation currents along the magnetic field lines, which break the magnetic topology of the nested flux surfaces of a tokamak equilibrium. The new topology leads to a thermal short-circuit across the island width, which degrades the energy confinement of the plasma. Magnetic islands can have several driving terms. They can arise from the free energy of an unstable current profile. The growth of the island is then proportional to the tearing parameter Δ', given by the jump in the logarithmic derivative of the radial magnetic field [1]. In contrast to these "conventional" tearing modes, neoclassical tearing modes (NTMs) are driven by a helical perturbation of the bootstrap current, which is generated by the local flattening of the pressure profile across an existing island [2]. Since the island growth increases with increasing plasma pressure, neoclassical tearing modes can have important repercussions on the confinement in high performance discharges.

The evolution of the full radial island width, w, is described by the generalized Rutherford equation [3],

$$\frac{\tau_R}{r_s}\frac{dw}{dt} = r_s\Delta'(w) + r_s\beta_p\Big(- \frac{\hat{a}_{GGJ}}{\sqrt{w^2+0.2w_d^2}} + a_{bs}\frac{w}{w^2+w_d^2} - \frac{\hat{a}_{pol}}{w^3}\,h(w)\Big) \qquad (1)$$

where τ_R is the resistive time at the resonant flux surface which has a radius r_s and β_p is the poloidal beta. The first two terms on the right hand side of Eq. (1) describe the conventional driving mechanism. The tearing parameter Δ' decreases with increasing island width [4],

$$\Delta'(w) = \Delta'(0) - \alpha w. \qquad (2)$$

The Glasser-Green-Johnson term ($\hat{a}_{GGJ}$) comprises the usually stabilizing effect of toroidicity [5]. This curvature effect is modified by a finite perpendicular diffusion scale length $w_d = 5.1 r_s (R/(r_s n s_s))^{1/2}(\chi_\perp/\chi_\parallel)^{1/4}$ [6], with R being the major radius, n the toroidal mode number and s_s the magnetic shear on the resonant flux surface. The island growth of a dominantly current driven tearing mode is shown in Fig. 1(a). The destabilizing effect of the perturbed bootstrap current is described in the third term (a_{bs}) [2]. An incomplete flattening of the pressure profile caused by the finite perpendicular diffusion scale length w_d reduces the perturbation of the bootstrap current for small islands [7]. The fourth term ($\hat{a}_{pol}$) accounts for the polarization current, which arises from the ion inertial response to the rotation of the island. Its sign depends on the island rotation frequency with respect to the electron and ion diamagnetic drift frequencies [8]. The factor $h(w)$ accounts for its behavior for w smaller than the ion banana width, which is the limit of validity of the polarization

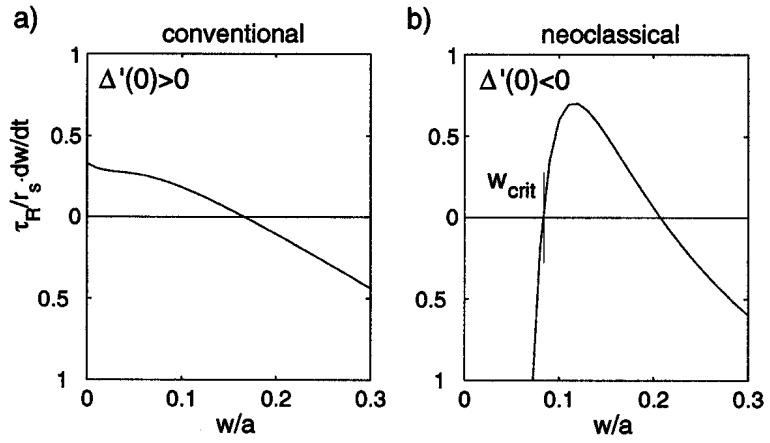

FIG. 1: Island growth of (a): a dominantly current driven and (b): a neoclassical tearing mode assuming a stable current profile.

current model. The island width evolution of an NTM, characterized by a large bootstrap current and assuming a stable current profile, $\Delta' < 0$, is shown in Fig. 1(b).

Since the neoclassical drive of an island is reduced by the effects of an incomplete flattening of the pressure profile and, possibly, polarization currents, an NTM requires a seed island whose width has to exceed a critical island width w_{crit} for a positive growth, Fig. 1(b). It is therefore possible to exceed the critical beta while staying metastable with respect to the neoclassical mode as long as no sufficiently large seed island is present. Such seed islands are usually provided by sawteeth, fishbones or ELMs [9–13].

In the TCV tokamak ($R = 0.88\,\mathrm{m}$, $a = 0.25\,\mathrm{m}$, $B \leq 1.54\,\mathrm{T}$), neoclassical tearing modes are observed in discharges with additional electron cyclotron heating (ECH). The NTMs have so far only been identified in discharges in which a tangential component of the wave vector with respect to the magnetic field leads to electron cyclotron current drive (ECCD). Typically $1 - 1.5\,\mathrm{MW}$ of ECH power is injected for electron cyclotron current drive in the direction of the Ohmic plasma current (co–ECCD) in the plasma center. The plasma current is low, corresponding to edge safety factors q_a from 7 to 9. The applied co–ECCD and the high safety factor lead to particularly peaked temperature and current profiles. The central electron density at the onset of the modes ranges from 1.2 to $3.0 \times 10^{19}\mathrm{m}^{-3}$ and is only limited by runaway electrons at low densities and by refraction of the microwave beam at higher densities. At the onset of the NTM the electron collisionality normalized to the banana bounce frequency, $\nu_{\mathrm{e}}^{\star} = \nu_{\mathrm{e}}/\omega_{\mathrm{b}}$, is low, ranging from 0.01 to 0.06. Owing to the ECH

heating scheme, the ion temperature remains low. The ion collisionality normalized to the electron diamagnetic drift frequency $\nu_* = \nu_i/(m\epsilon\omega_{e*})$ has values in the range from 0.1 to 0.5, where the polarization current is typically expected to become important. The poloidal ion Larmor radius remains approximately constant, $\rho_p \approx 2.6\,\mathrm{cm}$. The normalized beta β_N ranges from 0.4 to 0.8. These parameters are similar to those observed at the onset of NTMs in other tokamaks with dominant electron heating, such as COMPASS-D [12] and T-10 [13]. Under these conditions the mode can become unstable after a few $10\,\mu\mathrm{s}$ or even after more than 1 s after the start of the additional heating power.

In discharge #15963, shown in Fig. 2, two gyrotrons were switched on at t=0.4 s. About 300 ms later an MHD mode starts to grow with a growth time of the order of 10 ms and saturates at a high amplitude. The degradation of the energy confinement is clearly visible on the central soft X-ray emissivity. At t=1.95 s one gyrotron switches off. The amplitude of the mode decreases with the decreased additional heating power. After the switch-off of the last gyrotron the amplitude decreases to zero.

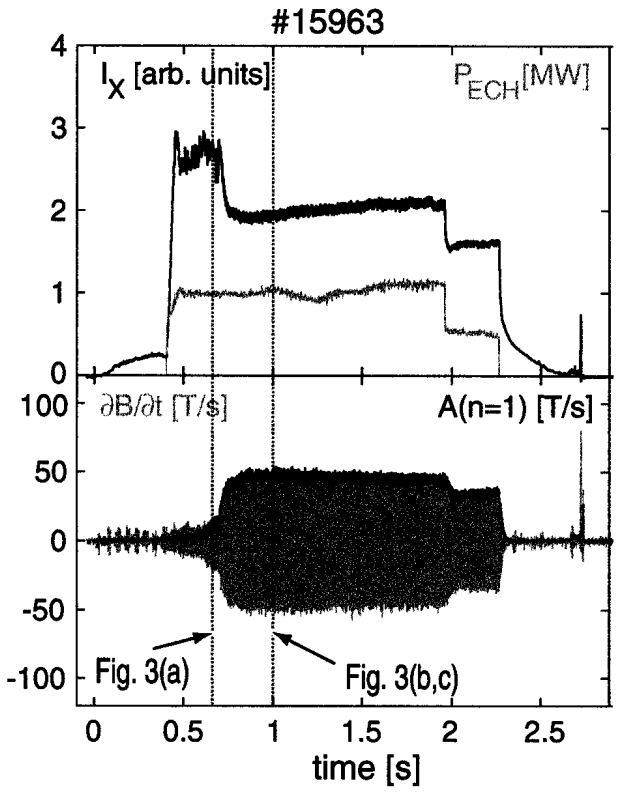

FIG. 2: During ECH a drop in the line integrated soft X-ray intensity along a central chord I_X is caused by a large amplitude $n = 1$ mode seen in the magnetic fluctuation measurements.

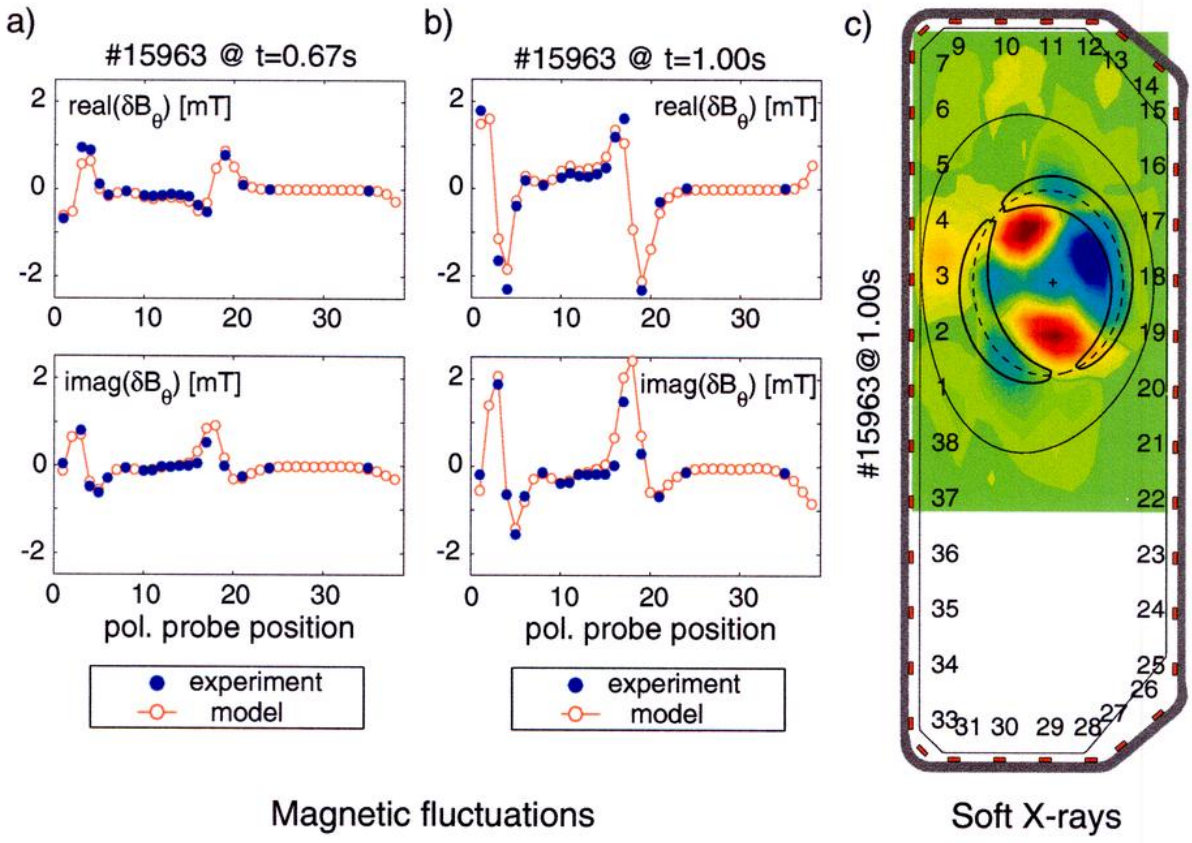

FIG. 3: In discharge #15963, Fig. 2, the mode structure in the initial phase (a) and during saturation (b) is in good agreement with the modeled 2/1 island. (c): The superposition of the equilibrium and perturbation flux reveals the island geometry. The $m = 2$ is also seen in the SVD of the tomographically reconstructed soft X-ray emissivity.

The mode structure is determined from magnetic fluctuations and soft X-ray emissivity measurements. A toroidal array of magnetic pick-up probes identifies a dominant n=1 mode, Fig. 2. This mode rotates at 4 to 5 kHz in the direction of electron diamagnetic drift. Its poloidal structure is measured with an array of 38 magnetic pick-up coils in one poloidal plane, Fig. 3. Owing to the highly elongated vacuum vessel and the great flexibility of the plasma shape, the interpretation of the measurements requires an inversion. The inversion method used is based on a model of a force- and divergence-free perturbation current along the equilibrium field lines on a resonant surface [14]. A Biot-Savart integration, using the modeled perturbation current distribution, reveals the eddy currents in the vacuum vessel and, including the latter, also the magnetic field at the location of the pick-up coils. A comparison of the phase and amplitude of the modeled and measured mode structures

identifies an m=2 mode, Fig. 3(a,b). The fitted amplitude also yields the assumed total perturbation current, which can be used to compute the helical flux of the perturbation. A superposition of the perturbed and equilibrium helical flux results in an island size of 20% of the minor radius corresponding to 4 cm on the outboard mid-plane, Fig. 3(c). The mode is also seen in the tomographic reconstruction of soft X-ray emission measurements along 200 lines-of-sight. A singular value decomposition (SVD) of the reconstructed emissivity also reveals an m=2 mode, which rotates with the same frequency in the same direction as the magnetic measurements, Fig. 3(c).

In order to identify the driving term of the $m/n = 2/1$ island, the evolution of its width w is tested against the evolution of a solely neoclassically driven tearing mode according to the modified Rutherford equation (1) assuming $\Delta' < 0$. The values of $\beta_{\mathrm{p}}(t)$ are taken from the experiment. The evolution of the experimental island width w_{expt}, starting with the rapid growth at $t = 0.69\,\mathrm{s}$, which already corresponds to $w = 3\,\mathrm{cm}$, agrees well with the prediction w_{theor}, Fig. 4. At such an island width the stabilizing effects of perpendicular transport and polarization currents can be neglected and w_{d} and a_{pol} were simply set to zero. Since the conventional (Δ') and the neoclassical (a_{bs}) driving terms differ in their β_{p}

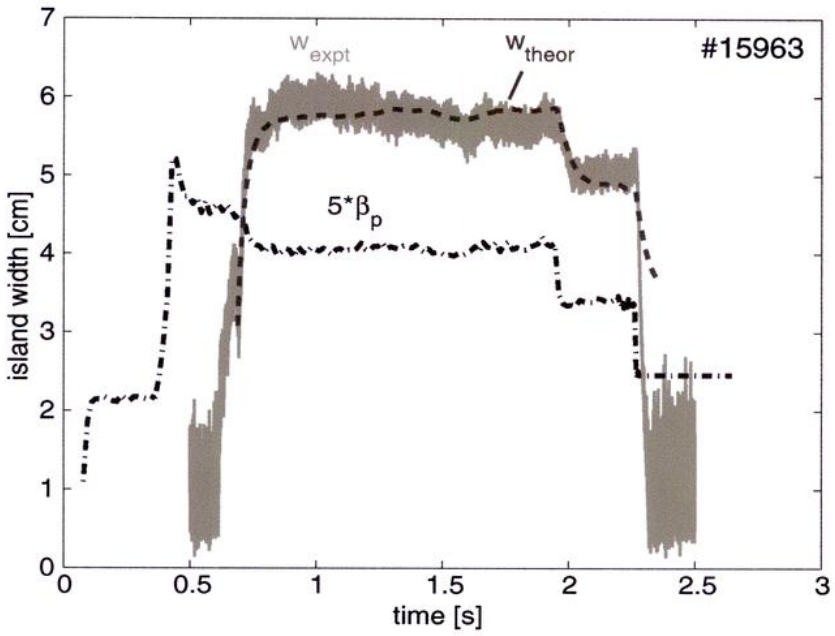

FIG. 4: The evolution of the island width of a 2/1 NTM according to Eq. (1), w_{theor}, using the experimental $\beta_{\mathrm{p}}(t)$ is in good agreement with the experimental island width w_{expt}, derived from magnetic measurements.

and w dependence, the observed mode clearly shows the characteristics of a neoclassical mode. The rapid change of the saturated island width after the switch-off of one gyrotron at $t = 1.95\,\mathrm{s}$ corresponds to the resulting change of β_p, which occurs on the fast confinement time scale ($\tau_E \sim 5\,\mathrm{ms}$), whereas Δ' can only change on a longer current diffusion time scale ($\tau_\mathrm{R} \sim 100\,\mathrm{ms}$). The simplifying assumptions, however, do not allow a satisfactory description of the island evolution for small values of w. The evolution at small w, in particular the seeding process, is analyzed in more detail.

The TCV plasmas, where neoclassical modes are observed, are in L-mode and consequently, ELM-free discharges. Owing to the high value of q_a and the central heating, they show no or only small sawteeth and they are also stable with respect to the fishbone instability. Hence, none of the common seeding mechanisms apply.

The onset of neoclassical tearing modes in TCV is investigated in detail by analyzing the evolution of the island width of the 2/1 NTM seen in #18458, Fig. 5(a). The measured growth of the island dw/dt, shown as a function of w in Fig. 5(c), clearly reveals two distinct growth phases. The faster growth at large w corresponds to the neoclassical island evolution previously modeled for #15963, Fig. 4. The critical island width is approximately $w_\mathrm{crit} = 2.8\,\mathrm{cm}$. It is suggested that the island growth up to w_crit is driven by the current profile. The 2/1 mode structure of the magnetic perturbation measurements does not show any significant differences between the two growth phases, Fig. 3(a,b). The initial growth of $0.4\,\mathrm{m/s}$ decreases as the conventional drive from Δ' decreases with w (Eq. (2)). The effect of Δ' is also visible after the switch-off of ECH, Fig. 5(b), when dw/dt drops with β on an energy confinement time scale ($\tau_E \sim 5\,\mathrm{ms}$) to the value determined by $\Delta'(w)$. At such large values of w, Δ' is strongly stabilizing, but slowly increases on a current diffusion time scale ($\tau_\mathrm{R} \sim 100\,\mathrm{ms}$), and, thereby, clearly exhibits the linear dependence of Δ' on w, Fig. 5(c).

In order to demonstrate that the observed growth can be caused by a conventional tearing mode destabilizing a neoclassical tearing mode, the right-hand-side of the modified Rutherford equation (1) has been modeled to reproduce the distinctive features of Fig. 5(c). The used parameters a_GGJ, a_bs, a_pol and w_d correspond within their error bars to the values predicted from the measured profiles of #18458 according to the expressions given in [3]. Owing to the low collisionality, the scale length w_d was determined using the convective form of the parallel heat conductivity, $\chi_\parallel$ [7]. The modeling required a limitation of the polarization current effect at small island width. This was achieved by choosing $h(w) = w^4/(w^4 + w_0^4)$

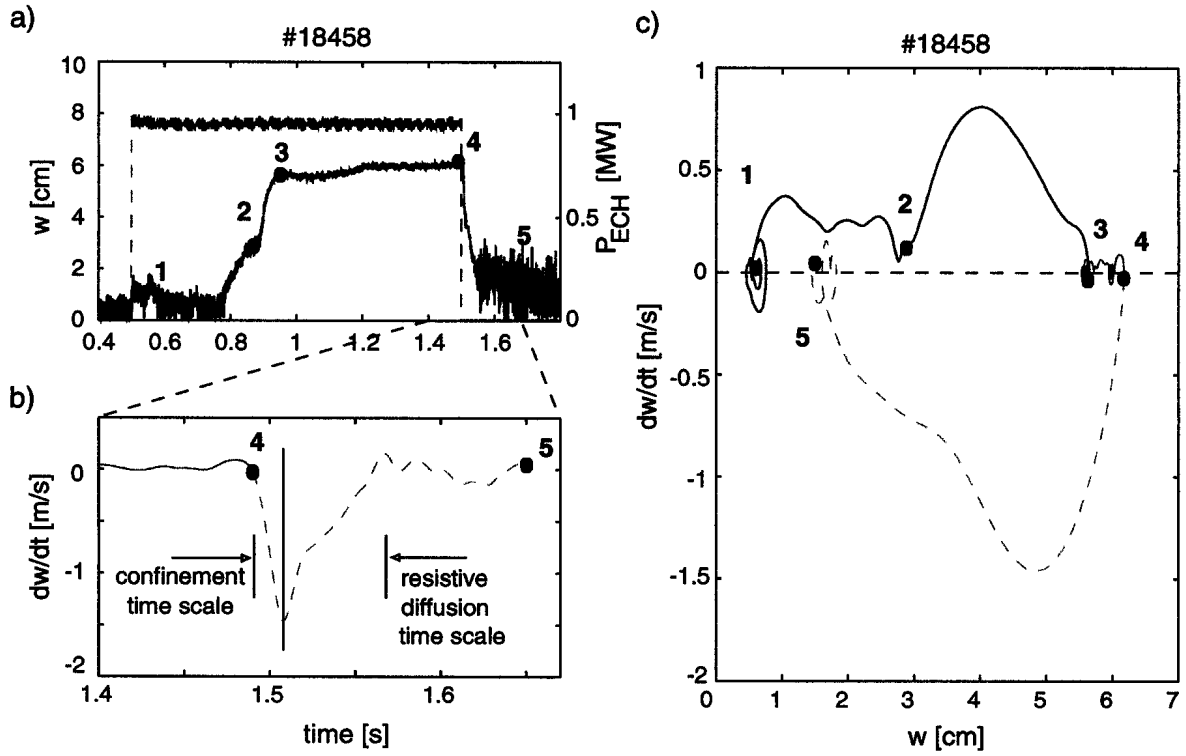

FIG. 5: (a): A current driven tearing mode grows on a slow time scale and approaches saturation (1→2). Once w exceeds w_{crit}, the mode grows on a faster time scale to its full width (2→3). (b): After the ECH is switched off (4) the neoclassical driving term decays on a fast confinement time scale, whereas the conventional tearing mode stability evolves on a slower current diffusion time scale. (c): The experimental island growth dw/dt is shown as a function of w.

with $w_0 \sim \sqrt{\epsilon} w_{\mathrm{p}}$, which essentially leads to a suppression of neoclassical effects at small w. Since the current profile is not known with a sufficient accuracy the tearing parameters $r_s \Delta'(0) = 1$ and $\alpha = 35\,\mathrm{m}^{-2}$ were also fitted. Then the predicted island growth, Fig. 6, indeed reproduces the features of the observed island growth in Fig. 5(c).

The destabilization of a neoclassical mode by a conventional tearing mode elucidates the occurrence of NTMs in "triggerless" TCV discharges. It also explains the peculiar conditions under which NTMs are observed in TCV, since the initial current profile must also be unstable with respect to conventional tearing modes.

TCV results provide the first clear observation of the transition from a mainly conventionally driven island to a neoclassical island evolution as current and pressure profiles evolve. Such a destabilization mechanism can explain the occurrence of apparently "triggerless" NTMs observed in other experiments [9, 13]. The experiment shows both, the linear de-

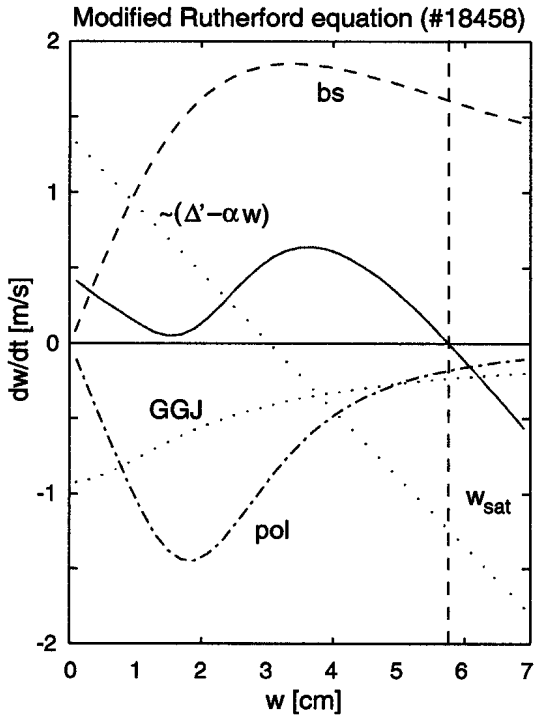

FIG. 6: The experimental island growth dw/dt, Fig. 5(c), is well reproduced by the r.h.s. of Eq. (1). The values used, $\beta_p = 0.75$, $a_{\rm GGJ} = 0.1$, $a_{\rm bs} = 0.7$, $a_{\rm pol} = 2\,cm^2$ and $w_d = 3.5\,{\rm cm}$, correspond to the values predicted from the measured profiles [3]. The parameters $r_s\Delta'(0) = 1$ and $\alpha = 33\,{\rm m}^{-2}$ are fitted.

pendence of Δ' on w, while the island is mainly current driven, and the dependence of its saturated width on β, while it is neoclassically driven. The entire growth of the island is found to be well described by the modified Rutherford equation (1), where the evolution of Δ', the neoclassical drive at large w and its assumed suppression at small w are important and relevant.

ACKNOWLEDGMENTS

It is a pleasure to acknowledge the excellent support of the whole TCV team. This work was partly funded by the Fonds National Suisse de la Recherche Scientifique.

REFERENCES

[1] H. P. Furth, P. H. Rutherford, and H. Selberg, Phys. Fluids **16**(7), 1054 (1973).

[2] R. Carrera, R. Hazeltine, and M. Kotschenreuther, Phys. Fluids **29**(4), 899 (1986).

[3] O. Sauter et al., Phys. Plasmas **4**(5), 1654 (1997).

[4] R. B. White, D. A. Monticello, M. N. Rosenbluth, and B. V. Waddell, Phys. Fluids **20**(5), 800 (1977).

[5] A. H. Glasser, J. M. Greene, and J. L. Johnson, Phys. Fluids **18**(7), 875 (1975).

[6] H. Lütjens, J.-F. Luciani, and X. Garbet, Phys. Rev. Lett. (2002), accepted for publication.

[7] R. Fitzpatrick, Phys. Plasmas **2**(3), 825 (1995).

[8] J. Connor, F. Waelbroeck, and H. Wilson, Phys. Plasmas **8**(6), 2835 (2001).

[9] A. Gude, S. Günter, S. Sesnic, and ASDEX Upgrade team, Nucl. Fusion **39**(1), 127 (1999).

[10] R. Buttery et al., in *Proc. 26th EPS Conf. on Controlled Fusion and Plasma Physics (Maastricht, 1999)*, edited by B. Schweer, G. Van Oost, and E. Vietzke (EPS, Mulhouse, 1999), vol. 23J, p. 121.

[11] R. La Haye, B. Rice, and E. Strait, Nucl. Fusion **40**(1), 53 (2000).

[12] D. A. Gates et al., Nucl. Fusion **37**(11), 1593 (1997).

[13] D. Kislov et al., Nucl. Fusion **41**(11), 1619 (2001).

[14] M. Schittenhelm, H. Zohm, and ASDEX Upgrade team, Nucl. Fusion **37**(9), 1255 (1997).